AIChE

Relationship Between the Size of Mist Droplets and Ethanol Condensation Efficiency at Ultrasonic Atomization on Ethanol–Water Mixtures

Hitomi Kobara, Makiko Tamiya, and Akihiro Wakisaka
Research Institute for Environmental Management Technology, National Institute of Advanced Industrial Science and Technology (AIST), Onogawa 16-1, Tsukuba, 305-8569, Japan

Tetsuo Fukazu and Kazuo Matsuura
Laboratory of Separation through Atomization (LSA), Ikenotani, Ooasacho, Naruto, Tokushima, 779-0303, Japan

DOI 10.1002/aic.12008
Published online August 24, 2009 in Wiley InterScience (www.interscience.wiley.com).

High-frequency (2.4 MHz) ultrasonic irradiation to an ethanol–water mixture can induce the generation of ethanol-rich mist droplets at lower temperatures. Two groups of droplets in micrometer- and nanometer-sized were observed in the mist generated by the ultrasonic atomization. Nanosized droplets were considered to be ethanol-rich droplets which cause ethanol condensation. © 2009 American Institute of Chemical Engineers *AIChE J,* 56: 810–814, 2010
Keywords: ultrasonic atomization, ethanol-rich liquid droplet, size distribution

Introduction

When a liquid is irradiated with ultrasound, a capillary fountain jet arises from the surface of the liquid and mist droplets are generated from the fountain jet. This is called ultrasonic atomization and is used as a method of easily obtaining liquid particles.

The mist produced by the ultrasonic atomization of an ethanol–water mixture has been collected and subjected to measurement of ethanol concentration. Analysis of the collected mist has revealed that the ethanol concentration in the mist is higher than that estimated through the gas–liquid equilibrium as shown in Figure 1.[1–3] It is interesting that the ethanol concentration in the mist particles becomes higher when the ultrasonic atomization was carried out at lower temperatures. An efficient separation/collection of ethanol is able to be carried out from low-concentration ethanol aqueous solution by dehydration of the mist using a molecular sieve.[4] This mist generation by ultrasonic atomization is nonthermal behavior, and the ultrasonic transducer consumes about 10% of the energy required for vaporization by heating. Therefore, this new separation process is expected to be useful because of its energy-saving features.

The ultrasonic ethanol condensation phenomenon has been discussed before in terms of the capillary wave produced on the surface of the liquid[5,6] and the evaporation from the liquid and the droplet surface.[7] Yano et al., through measurement of the diffraction pattern after X-ray irradiation of the capillary fountain jet, showed that the microscopic structure therein is not disturbed during the ultrasonic irradiation.[6] They also measured the size of the ethanol-rich droplets to be a diameter of 1 nm by small-angle X-ray scattering (SAXS), and they concluded that the ethanol-rich droplets were generated from the surface through the ultrasonic atomization.[8] Wakisaka and Matsuura have reported that the generation of the nanosized ethanol-rich droplets is related to the cluster structures of ethanol–water mixtures.[9]

It is still under discussion that generation mechanism of ethanol-rich mist droplets in this technique and how to raise the ethanol condensation efficiency. To solve these subjects,

Correspondence concerning this article should be addressed to H. Kobara at h-kobara@aist.go.jp

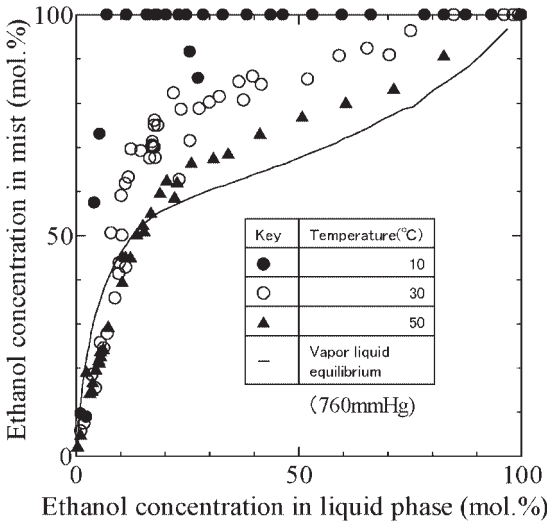

Figure 1. Ethanol separation characteristics of ethanol–water mixtures.

The horizontal axis is the ethanol concentration in ethanol–water mixtures and the vertical axis is the concentration of ethanol in the mist or vapor. The solid line indicates the vapor–liquid equilibrium of ethanol–water mixtures under 1013 hPa.[1,2]

it is necessary to measure size distribution of droplets over a wide range. Here, we tried to measure mist droplet sizes by scanning mobility particle sizer (SMPS), which is increasingly being used to measure nanoscale atmospheric aerosol particles[10,11] and nanosized particles in materials,[12,13] and by light-scattering particle counter, which can be used to measure particles with a diameter of 300 nm or more. We would like to show the relation between the mist droplet size distribution from nanometer to micrometer and the ethanol condensation in those droplets.

Experiment

The experimental equipment used is shown in Figure 2. A 2.4 MHz ultrasonic transducer (HM-2412: Honda electrics) was attached to the bottom of a Pyrex glass columnar container, into which about 500 ml sample solution (0, 5, 20, 50 mol % ethanol in water) was poured. Ultrasound creates a fountain jet that rises to a height of 3–4 cm from the surface of the liquid, and mist droplets were scattered from the fountain jet into the air. The mist was introduced into the particle-size distribution meters described below with nitrogen gas. An ultrasonic transducer with a frequency of 2.4 MHz was running at 25 V and 0.7 A. The nitrogen gas carried the mist at 15 or 50 dm^3/min, and the temperature of the liquid was maintained at 10°C, 20°C, or 50°C.

The size of the resulting mist droplets was measured by two ways in dependence on the size region. The size regions 10–700 nm and 0.3–10 μm were measured by an SMPS MODEL 3936NL76-N (TSI) and a hand-held particle counter (HPC) (MODEL3016, LIGHTHOUSE), respectively. Both SMPS and HPC are based on the principle of particle detection by the light-scattering method. HPC can measure particles with a diameter of 0.3 μm or more by laser diode light scattering. Nanoparticles with a diameter smaller than the light wavelength cannot be detected directly by light scattering. On the other hand, the SMPS system initially sizes particles on the basis of their electric mobility. The resulting monodispersed particles are made to pass through a supersaturated butanol vapor, which causes them to grow into a size detectable by light scattering.

Results and Discussion

Effect of ethanol concentration in solution on mist size

Figure 3 shows the size distribution of ultrasound-generated mist droplets under the conditions of ethanol composition (a) 0%, (b) 5 mol %, and (c) 50 mol % in the mixtures. Nitrogen carrier gas flow rate was 15 dm^3/min and liquid temperature was 20°C. Two peaks in the particle size distribution were observed at around 30 nm and 1 μm in Figures 3a, b. Ultrasonic irradiation of water or a solution containing ethanol at low concentration clouded up the inside of the mist generator. This was because the mist included relatively large micrometer-size droplets that reflect visible light. Moreover, fine droplets of about 20–30 nm were generated at all measurements. It is confirmed that the ultrasonic atomization has function to disperse two types of liquid droplet, fine and coarse one.

Droplet size d_p is represented as $d_p = \alpha(\sigma/\rho F^2)^{1/3}$ by Lang,[14] which is derived from the Kelvin's theory, where α is the constant, σ is the surface tension, ρ is the liquid density, and F is the ultrasound frequency. d_p is calculated to be about 2.3 μm for water and 1.7 μm for ethanol, when 2.4 MHz oscillator is used. Count median diameter (CMD) of micrometer droplets is not able to be exactly determined because of low resolution of HPC; however, the distribution of micrometer droplets shows obvious peak at 1 μm. When ethanol is added into water, surface tension σ decreases and solution density ρ slightly decreases. Therefore, from Lang's equation, d_p is estimated to be decreased with increases the ethanol concentration in the solution. However, the size distribution of coarse droplets was not shifted to smaller side but the generation of droplets became hard when ethanol concentration in the solution increased from 0 to 50 mol %. As for nanosized droplets, the CMDs of droplets from 100% water, 5 mol % ethanol, and 50 mol % ethanol were 24.3, 30.2, and 33.1 nm, respectively. This tendency contradicts

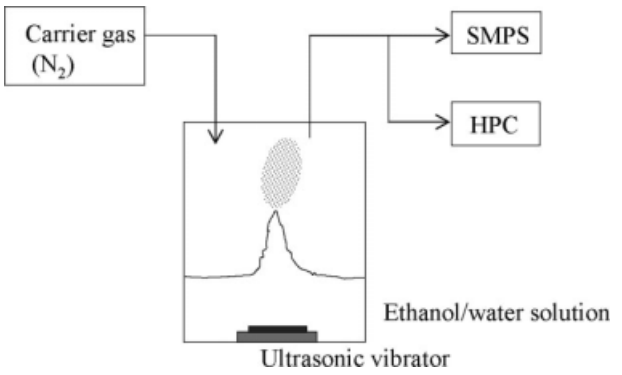

Figure 2. Schematic diagram of the experimental setup to generate mist droplets by ultrasonic atomization and the measurement equipment.

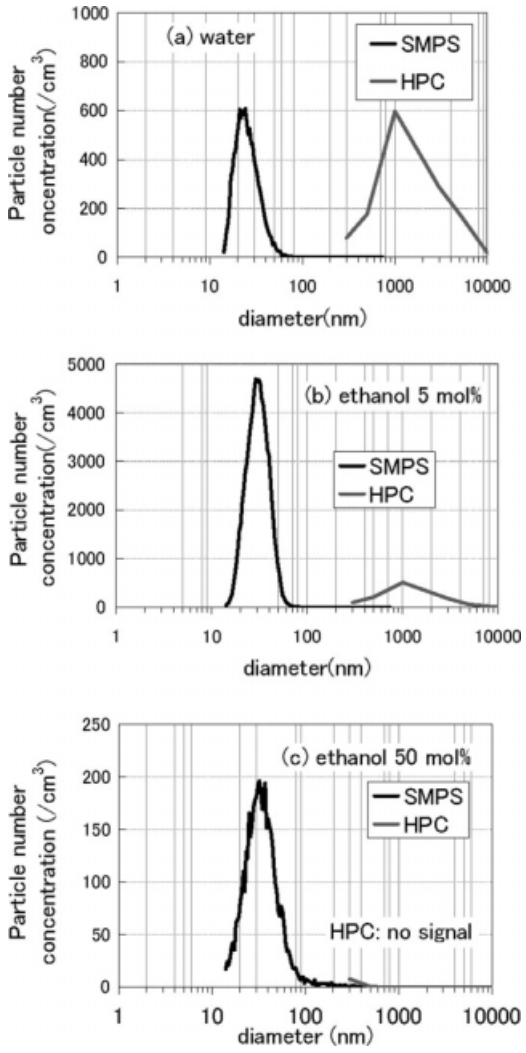

Figure 3. Particle size distribution of mist generated by ultrasonic irradiation of (a) water, (b) ethanol 5 mol %, and (c) ethanol 50 mol % at 20°C and carrier-gas flow rates of 15 dm^3/min.

the Lang's equation that d_p decreases with ethanol addition to the solution. Therefore, it is not able to be explained from Lang's equation why the coarse droplets disappeared with increase of ethanol concentration in the mixture. Lang's equation was derived for some experiments using oscillators of frequencies below 800 kHz. It should be noted that the Lang's equation does not consider the physical properties of solution nor ultrasound frequencies in case of high frequency over 1 MHz.

To explain these phenomena, a viewpoint of microscopic heterogeneous structure was considered. At very low ethanol concentrations (~5 mol %), the ethanol condensation efficiency by ultrasonic mist generation is lower than that expected according to a gas–liquid equilibrium curve.[1,2] The study on microscopic structures of ethanol–water mixtures through mass spectroscopy[9] showed that in a solution with a low ethanol concentration (~7 mol %), the ethanol molecules are widely delocalized in a hydrogen-bonding network of water molecules in which the ethanol molecules are existing as a part of this hydrogen-bonding network. When mist droplets are generated from this solution through the ultrasonic atomization, micrometer-size mist droplets are generated due to the strong hydrogen-bonding network of water molecules including ethanol molecules. Therefore, the ethanol concentration in the generated mist droplets is not high. When more ethanol is added to the solution, the self-association of ethanol is promoted. Because of this microscopic phase separation, the surface tension decreases remarkably. This means microscopic phase separation between an ethanol-rich and a water-rich cluster phase. The ultrasonic atomization to such a microheterogeneous solution leads to preferential atomization from the ethanol-rich cluster. For the ethanol–water mixtures, the ethanol-rich phase would be atomized preferentially, which forms fine mist droplets (10–100 nm). It should be noted that the ethanol concentration in the mist droplets (Figure 1) and the size distribution of the mist droplets generated by the ultrasonic irradiation (Figures 3b, c) are controlled by the cluster structures of ethanol–water mixtures depending on the mixing ratio.

Effect of solution temperature on mist size

Figure 4 shows the particle distribution of mist droplets generated by ultrasonic irradiation of a 20 mol % ethanol solution maintained at 10°C, 20°C, and 50°C. At 10 and 20°C, few coarse droplets (~1 μm) were generated and fine droplets (10–100 nm) predominated, whereas at 50°C, coarse droplets were apparently generated.

The liquid droplet size d_p is represented by Kelvin's equation including temperature T as follows; $d_p = 4\bar{v}\sigma/\mathrm{RTlnS}$,[15] where $\bar{v}$ is molecular volume, σ is surface tension, R is the gas constant, and S is supersaturation degree. This equation describes the relationship between liquid droplet and equilibrium vapor pressure based on the thermodynamic theory. The diameter d_p is estimated to be larger than 1 μm and d_p should be decreased with increasing T from this equation both for water and ethanol. As for fine nanosized droplets, CMDs of droplets at 10°C, 20°C, and 50°C were 41.9, 30.4, and 26.0 nm, respectively. The CMDs are shifted to smaller size and it corresponds to the equation quantitatively. However, coarse micrometer-sized droplets were not generated at 10°C and 20°C, but observed at 50°C. This is obviously contrary to the equation described earlier. Therefore, when the ethanol condensation process through the ultrasonic atomization is discussed, an alternative interpretation is needed rather than vapor equilibrium considering static interface between the liquid and the gas phase.

As shown in Figure 1, under the condition of 20 mol % liquid-phase ethanol, the ethanol condensation in the mist occurs at 10°C and 30°C, rather than nearly equivalent to the vapor–liquid equilibrium at 50°C. Moreover, the ethanol concentration in mist becomes higher with decreasing the temperature in the range that ethanol condensation occurs. This is remarkably contrastive to the fact that coarse micrometer-sized droplets are generated under the condition of low ethanol concentration in the mixture and high liquid temperature. Therefore, it is considered that ethanol is concentrated to fine nanosized droplets, whereas coarse micrometer-sized droplets are poor in ethanol.

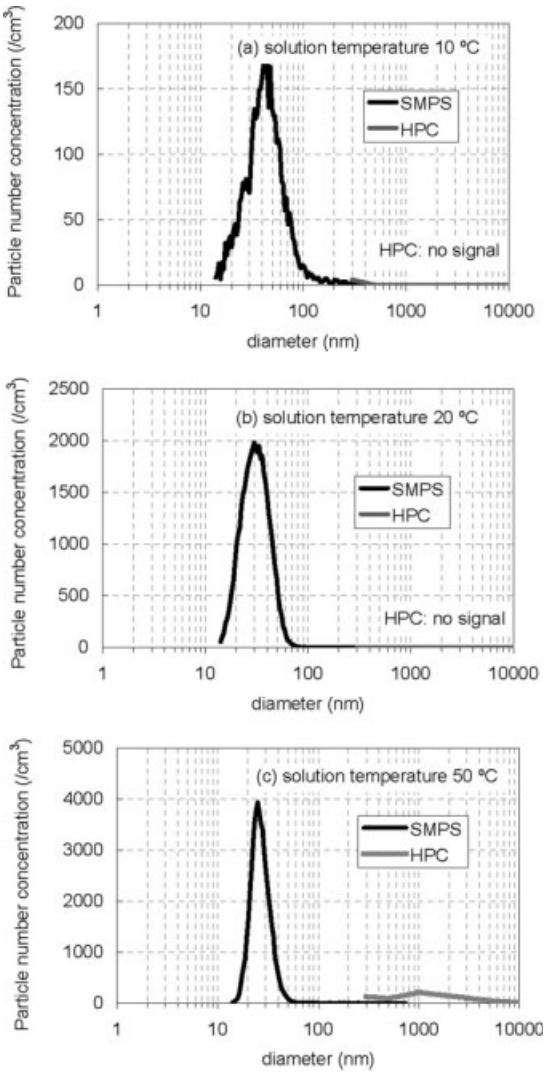

Figure 4. Solution temperature dependence of size distribution of mist droplets generated by ultrasonic irradiation of 20 mol % ethanol solution.

Carrier gas flow rate was 15 dm^3/min and solution temperatures were (a) 10°C, (b) 20°C, and (c) 50°C.

The effect of solution temperature on the size of mist droplet and on the ethanol concentration in the mist droplets also indicates that ethanol is concentrated in the fine mist droplets (10–100 nm) generated predominantly at lower temperatures. The observed temperature effects on the mist droplet size and on the ethanol concentration in the mist droplets are also related to the microscopic phase separation at the cluster level in the solution. It has been reported that the microscopic phase separation between ethanol-rich and water-rich clusters took place more significantly at lower temperatures.[9] On the basis of the mass spectrometric analysis of clusters in ethanol–water binary mixtures, the ethanol self-association clusters were mainly observed at lower temperatures, on the other hand, these ethanol self-association clusters interacted with surrounding water-rich clusters at higher temperatures. This means that the microscopic phase separation is promoted at lower temperatures. The observed temperature effect also indicates that the ethanol-rich clusters are transferred from the liquid to the mist with 10–100 nm size by the ultrasonic atomization.

Yano et al. measured the size of the mist droplets generated by the same kind of ultrasonic atomization for ethanol–water mixtures, by means of the small angle X-ray scattering (SAXS).[8] They observed effects of ethanol concentration and temperature in ethanol–water mixtures on the size of mist droplets generated by the ultrasonic atomization. The results obtained by their SAXS measurements are strongly correlated with these results. Yano et al. also suggested that the size of the mist droplets were quite different between the ethanol-rich mist droplets and the water-rich droplets. The sizes of the ethanol-rich and the water-rich droplets were $\lesssim 1$ nm and ~ 100 nm, respectively. This trend is similar to our result despite a difference in absolute diameter.

SAXS and SMPS differ mostly in their time resolution. SAXS represents "in situ analysis," in which mist is spectroscopically observed directly. In contrast, in SMPS, droplets are separated according to size on the basis of their electric mobility and need to go through the step of being counted in order; therefore, even if the droplets could be sampled directly after their generation, a time lag of tens of seconds is inevitable. The diameters of both ethanol-rich and water-rich droplets, as measured by SMPS, are shifted toward larger values than are obtained by SAXS, presumably because secondary products resulting from the association or

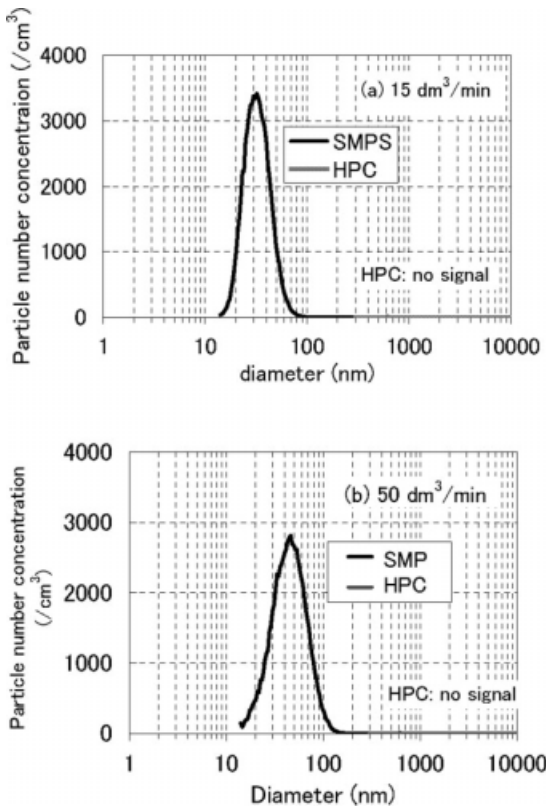

Figure 5. Size distribution of mist droplets generated by ultrasonic irradiation of 20 mol % ethanol solution under the conditions of carrier gas flow rate was (a) 15 dm^3/min and (b) 50 dm^3/min.

diffusion of instable ultrafine droplets are measured during SMPS. HPC is a very simple measurement system that can directly detect scattered laser light. Therefore, measurements obtained by HPC can be considered to be obtained under the same conditions as with SAXS. The production of water-rich droplets generated at high solution temperatures can be considered to peak at a particle diameter of 1 μm.

Effect of carrier-gas flow rate

We used carrier-gas flow rates of 15 and 50 dm^3/min to compare behavior of droplet dispersion at 20°C. Figure 5 shows the particle size distribution generated under the condition of carrier gas flow rate of 15 and 50 dm^3/min on 20 mol % ethanol solution. When the carrier gas flow rate was increased from 15 to 50 dm^3/min, no micrometer-sized coarse droplets were generated, and the size of the fine nanosized droplets tended to increase, from 32.0 to 44.4 nm of CMD. The more contact between the gas–liquid interface the easier the generation of droplets. This means that the flow of carrier gas plays a role in helping the transfer of liquid droplets from the interface to the gas phase.

The volume of the nanosized droplets dispersed per 1 min irradiation was 14.9×10^{12} nm^3 under the condition of 20°C and 15 dm^3/min, and was 39.4×10^{12} nm^3 at 20°C and 50 dm^3/min. Fine nanosized droplets, namely ethanol-rich droplets, were increased with increasing carrier-gas flow rate, which result in the increase of the ethanol condensation efficiency.

It is confirmed that Kelvin's equation is not applied to the ultrasonic atomization from experiments under the conditions of various liquid-phase ethanol concentration and temperature. The pattern of distribution of dispersed droplets is maintained at different carrier-gas flow rate; therefore, the size of droplets is mainly controlled by the composition and temperature of the solution, and the total quantity of recovered ethanol depends on the gas flow rate.

Conclusion

It was revealed that the ethanol condensation took place in the nanosized droplets generated from ethanol–water binary mixtures through the ultrasonic atomization under various liquid composition and temperature. Generation mechanism of mist droplets does not follow classical Kelvin's equation, and aggregates, reflecting the microscopic heterogeneous structure in solution, are dispersed into the gas phase. Dispersion of associated aggregates needs lower energy than the vaporization which takes molecules to pieces over the solution. Mist generation by ultrasonic atomization represents a less energy-consuming and highly efficient substance-separation process with great potential and can be used for fractionation of not only ethanol but also isopropyl alcohol and gasoline. This ultrasonic atomization has also been considered for condensation of bioethanol, which has recently attracted attention as new fuel.[16] Hopefully, the process will be useful as an energy-saving separation and condensation technology with great potential and will provide a breakthrough in ultrasonic technology.

Acknowledgments

This work was supported by a grant from the New Energy and Industrial Technology Development Organization of Japan.

Literature Cited

1. Matsuura K, Kobayashi M, Hirotsune M, Sato M, Sasaki H, Shimizu K. New separation technique under normal temperature and pressure using an ultrasonic atomization. *Jpn Soc Chem Eng Symp ser*. 1995; 46:44–49.
2. Sato M, Matsuura K, Fujii T. Ethanol separation from ethanol-water solution by ultrasonic atomization and its proposed mechanism based on parametric decay instability of capillary wave. *J Chem Phys*. 2001;114:2382–2386.
3. Matsuura K, Sato M, Sasaki H. Separation apparatus using ultrasonic atomization under low temperature and liqure making method using its apparatus. Jpn. Pat. 3822267, June 30, 2006.
4. Matsuura K, Fukazu T, Abe F, Sekimoto T, Tomishige T. Efficient separation coupled with ultrasonic atomization using a molecular sieve. *AIChE J*. 2007;53:737–740.
5. Kirpalani DM, Toll F. Revealing the physicochemical mechanism for ultrasonic separation of alcohol-water mixtures. *J Chem Phys*. 2002;117:3874–3877.
6. Yano YF, Douguchi J, Kumagai A, Iijima T, Tomida Y, Miyamoto T, Matsuura K. In situ X-ray diffraction measurements of the capillary fountain jet produced via ultrasonic atomization. *J Chem Phys*. 2006;125:174705:1–4.
7. Nii S, Matsuura K, Fukazu T, Toki M, Kawaizumi F. A novel method to separate organic compounds through ultrasonic atomization. *Chem Eng Res Des*. 2006;84:412–415.
8. Yano YF, Matsuura K, Fukazu T, Abe F, Wakisaka A, Kobara H. Small-angle X-ray scattering measurement of a mist of ethanol nanodroplets: an approach to understanding ultrasonic separation of ethanol-water mixtures. *J Chem Phys*. 2007;127:031101:1-4.
9. Wakisaka A, Matsuura K. Microheterogeneity of ethanol-water binary mixtures observed at the cluster level. *J Mol Liq*. 2006;129:25–32.
10. Mathis U, Mohr M, Kaegi R, Bertola A, Boulouchos K. Influence of diesel engine combustion parameters on primary soot particle diameter. *Environ Sci Technol*. 2005;39:1887–1892.
11. George IJ, Vlasenko A, Slowik JG, Broekhuizen K, Abbatt JPD. Heterogeneous oxidation of saturated organic aerosols by hydroxyl radicals: uptake kinetics, condensed-phase products, and particle size change. *Atmos Chem Phys*. 2007;7:4187–4201.
12. Lenggoro IW, Widiyandari H, Hogan CJ, Biswas P, Okuyama K. Colloidal nanoparticle analysis by nanoelectrospray size spectrometry with a heated flow. *Anal Chim Acta*. 2007;585:193–201.
13. Jung JH, Oh HC, Noh HS, Ji JH. Metal nanoparticle generation using a small ceramic heater with a local heating area. *J Aerosol Sci*. 2006;37:1662–1670.
14. Lang RJ. Ultrasonic atomization of liquids. *J Acoust Soc Am*. 1962; 34:6–8.
15. Friedlander SK. *Smoke, Dust and Haze*. John Wiley & Sons, Inc., 1977:230.
16. Gerald O. Purifying ethanol without distillation, Chementator, news. *Chem Eng*, January 1, 2006.

Manuscript received Dec. 16, 2008, and revision received Apr. 30, 2009.